IOPscience iopscience.iop.org

Home Search Collections Journals About Contact us My IOPscience

Electrical and optical properties of amorphous indium oxide

This article has been downloaded from IOPscience. Please scroll down to see the full text article.

1990 J. Phys.: Condens. Matter 2 6207

(http://iopscience.iop.org/0953-8984/2/28/011)

View the table of contents for this issue, or go to the journal homepage for more

Download details:
IP Address: 171.66.16.103
The article was downloaded on 11/05/2010 at 06:01

Please note that terms and conditions apply.

J. Phys.: Condens. Matter 2 (1990) 6207–6221. Printed in the UK

Electrical and optical properties of amorphous indium oxide

J R Bellingham, W A Phillips and C J Adkins
Cavendish Laboratory, Madingley Road, Cambridge CB3 0HE, UK

Received 8 February 1990, in final form 26 April 1990

Abstract. We present a detailed analysis of the electrical and optical properties of amorphous transparent conducting thin films of indium oxide prepared by ion beam sputtering with a wide range of carrier concentrations. We show that the resistivity is dominated by ionised impurity scattering despite the amorphous structure of the films. The weak effect of the structural disorder is confirmed by studies of the interband absorption and is explained by a consideration of the relative length scales of the structural disorder and the Fermi wavelength.

1. Introduction

It has been known for many years that indium oxide, in thin film form, is a transparent conductor, typically passing over 90% of visible light and displaying electrical resistivity between 10^{-5} and $10^{-6}\ \Omega$ m. These properties have led to a wide range of technical applications both in coating glass for energy-efficient windows or burglar alarms and as transparent elements in optoelectronic devices such as solar cells.

Physically these properties result from its being an n-type semiconductor with a band gap of between 3.5 and 4 eV. Oxygen vacancies provide electrons by acting as doubly charged donors, and films are generally sufficiently oxygen deficient that the electron gas in the conduction band is degenerate. Films are often prepared with a small proportion (5 to 15%) of tin oxide to form indium tin oxide (ITO) as this has been observed to increase the carrier concentration. The tin is commonly believed to provide electrons by substituting for indium and acting as a singly charged donor on an indium site.

The complex unit cell of crystalline In_2O_3 which contains 80 atoms has precluded band structure calculations. The properties are therefore discussed in terms of an assumed band structure consisting of a isotropic parabolic conduction band with an effective mass of between 0.30 and 0.35 m_e, a value derived from optical measurements (see, e.g., Szczyrbowski *et al* 1986). There is little information on the form of the valence band.

Most previous studies (reviewed by Hamberg and Granqvist 1986) have concentrated on polycrystalline films prepared on heated substrates. It is, however, possible to produce amorphous films with similar properties by ion beam sputtering onto room temperature substrates. These films clearly have enormous potential for transparent conducting coatings on heat-sensitive substrates. The aim of this paper is to explore the basic physics of these important films, which has received little attention in the past.

0953-8984/90/286207 + 15 $03.50 © 1990 IOP Publishing Ltd

After characterising the structure of the films, the electrical properties are discussed in terms of the various scattering mechanisms which contribute to the resistivity. Complementary optical studies of both the interband absorption and the plasma effects in the infra-red are used to complete a consistent picture of the electron gas in these films.

It is worth noting that the basic physics of even polycrystalline indium oxide is still open to question since such attempts as there have been to analyse the scattering mechanisms or the precise role of the tin have been inconclusive. The analysis of the amorphous films presented here is therefore highly relevant to our understanding of the polycrystalline variety.

2. Preparation and structural characterisation

The samples were prepared in an Oxford Instruments cryopumped ion beam sputtering system which has a base pressure around 10^{-8} mbar. The substrate is water cooled, remaining at room temperature for all the depositions described in this paper. By sputtering an indium target with an argon beam in the presence of a variable background pressure of oxygen, it has been possible to produce films ranging from pure indium metal to stoichiometric transparent insulating indium oxide. The pure metal is produced with no oxygen, after which increases in the oxygen pressure produce, successively, a shiny metal/oxide composite of resistivity around 10^{-5} Ω m, a brown opaque phase of resistivity typically 10^{-4} Ω m, a conducting transparent phase with resistivities as low as 5×10^{-6} Ω m, finally followed by the insulating transparent phase as the oxygen vacancies are removed. This sequence of phases is similar to that observed by Hebard and Nakahara (1982) who performed a similar experiment. The transparent conducting films that are the subject of this paper were prepared at deposition rates of typically 0.1 nm s^{-1} and at oxygen pressures of typically 2×10^{-4} mbar. Variation of this pressure within the range that would produce conducting transparent films allowed control of the electron density, consistent with the standard picture that the free electrons result from the presence of oxygen vacancies.

Structural characterisation of these films by both transmission electron microscopy and x-ray diffraction showed that they were entirely amorphous, with no evidence for a microcrystalline structure. An optical densitometer trace of an electron diffraction pattern negative was also taken. After subtraction of the background this provides an estimate of the structure factor $S(Q)$ which is shown in figure 1. The overall appearance of this plot, with a first peak at 23 nm^{-1}, is broadly similar to measurements on amorphous metallic alloys (Sadoc and Wagner 1983) with first peaks at q-values between 24 and 30 nm^{-1}. The width of the peak is also similar to those reported by Sadoc and Wagner. This structure factor is distinctly different from those of amorphous SiO_2 or the chalcogenide glasses in that it does not display a peak at low Q (between 10 and 15 nm^{-1}) which results from the tetrahedral structure of these glasses.

3. Electrical properties

The electrical properties of the films were assessed by resistivity and Hall effect measurements made at room temperature. Some measurements were also made at temperatures down to 4.2 K. The room temperature results are shown for all measured films in figure 2. Knowledge of the electron concentration allows calculation of the degeneracy temperature of the electron gas T_D given by

$$k_B T_D \simeq (\hbar^2/2m^*)(3\pi^2 n)^{2/3} = \varepsilon_F$$

where m^* is the effective mass in the model of a parabolic conduction band, and n is the

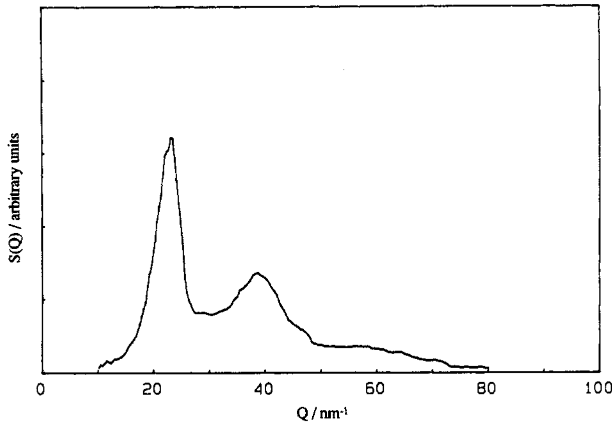

Figure 1. Approximation to the structure factor of the amorphous indium oxide, extracted from electron diffraction photographs.

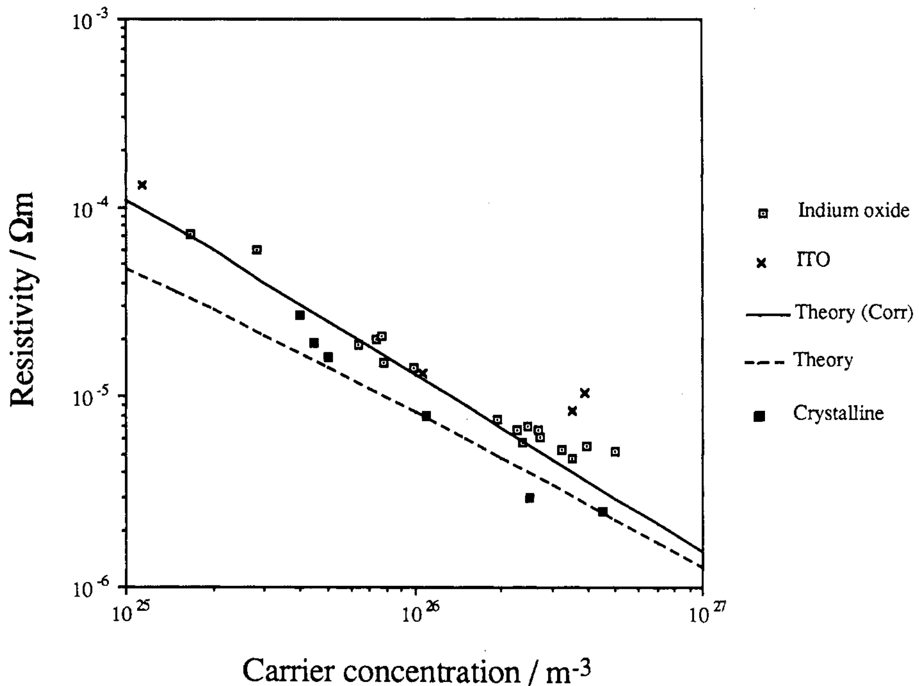

Figure 2. Room temperature resistivity and carrier concentration for all films on which measurements were made. Films prepared from the 9% Sn target are shown as ITO. The original calculation is based on the work of Dingle; the corrected one is based on that of Moore. Crystalline data are taken from Noguchi and Sakata (1980), Pan and Ma (1980), Chen *et al* (1983), Ovadyahu *et al* (1983) and Hamberg and Granqvist (1986).

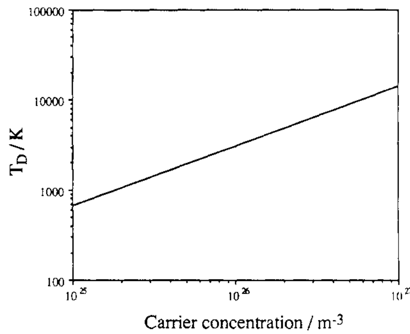

Figure 3. Degeneracy temperature as a function of carrier concentration.

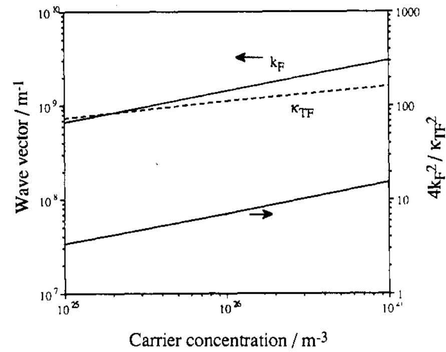

Figure 4. Plots of k_F, κ_{TF} and $4k_F^2/\kappa_{TF}^2$ against carrier concentration.

electron concentration. T_D is shown in figure 3, calculated for an effective mass of 0.3 m_e (see the optical results). It can be seen from a comparison of figures 2 and 3 that all the films prepared in this work have degeneracy temperatures well above room temperature. The degeneracy of these films was further confirmed by the temperature independence of the carrier concentration at temperatures between 300 and 4.2 K, and by the weak temperature dependence of the resistivity in the same region. (The resistivity at 4.2 K is typically 10% less than that at 300 K.)

Turning to the resistivities, these are some of the lowest reported for films made of pure indium oxide, without the addition of tin. The only films of significantly lower resistivity were the crystalline samples deposited on heated substrates by Pan and Ma (1980) and by Chen *et al* (1983). Lower resistivities, down to $1 \times 10^{-6}\ \Omega$ m, have been reported when tin has been added to form indium tin oxide (ITO), but only for crystalline films prepared on heated substrates. Attempts to ion beam sputter amorphous films of ITO onto room temperature substrates (Fan 1979, Aharoni *et al* 1986) have yielded resistivities between 6×10^{-6} and $8 \times 10^{-6}\ \Omega$ m, similar to the ITO films prepared in this work. The resistivities of the pure indium oxide films reported here are therefore the lowest of which we are aware for films deposited entirely at room temperature.

3.1. Ionised impurity scattering

In order to explain the observed resistivity of indium oxide it is necessary to consider carefully the mechanisms that may be scattering the electrons. The one mechanism that will certainly operate is scattering of the electrons by the ionised impurities, which must be present in order to preserve change neutrality. The scattering of conduction electrons by ionised impurities has been treated in the Born scattering approximation by Brooks (1955) and Dingle (1955). The work of Dingle will be discussed here.

The Born approximation gives an expression for the differential scattering cross section $I(\theta)$ which is defined as the fractional rate of scattering through an angle θ into unit solid angle when on average one particle of velocity v is incident in unit time.

$$\sqrt{I(\theta)} = \frac{2m}{\hbar^2 q}\int_0^\infty \sin(qr)|V(r)|r\,\mathrm{d}r.$$

$V(r)$ is the spherically symmetric scattering potential and q is the change in the electron wave vector. The scattering potential must take into account the screening effect of the free electrons; this is treated by Dingle in the Thomas–Fermi approximation, so that

$$V(r) = -(Ze^2/4\pi\varepsilon_0\varepsilon_r)\exp(-\kappa_{TF}r).$$

Here Z is the charge on the impurity, ε_r is the low-frequency relative permittivity and κ_{TF} is the Thomas–Fermi wave vector given by

$$\kappa_{TF}^2 = (3n/\pi^4)^{1/3}\, m^* e^2/\hbar^2\varepsilon_r\varepsilon_0.$$

In all the equations, n is used to denote the carrier concentration.

The low-frequency relative permittivity is the correct one to use as it is being used to describe the way the lattice screens out a static potential. For the case where there are N_i scattering centres per unit volume, the momentum relaxation time, τ, is related to the scattering cross section by

$$\frac{1}{\tau} = 2\pi N_i v \int_0^{\pi} (1-\cos\theta) I(\theta)\sin\theta\, d\theta$$

where v is the particle speed.

The equations above can be combined to give the relaxation time for an electron of wave vector $\boldsymbol{k}$ as

$$1/\tau(\boldsymbol{k}) = [N_i Z^2 e^4 m^*/8\pi(\varepsilon_0\varepsilon_r)^2\hbar^3 k^3] f(k) \quad (1)$$

where $f(k)$ is given by

$$f(k) = [\ln(1+\beta^2) - \beta^2/(1+\beta^2)]$$

and β is equal to $2k/\kappa_{TF}$.

For a degenerate system it is only necessary to consider the scattering of electrons at the Fermi surface, so the resistivity can be written as

$$\rho = [N_i Z^2 e^2 m^{*2}/24\pi^3(\varepsilon_0\varepsilon_r)^2\hbar^3 n^2] f(k_F). \quad (2)$$

To apply this calculation to indium oxide, values must be chosen for m^* and ε_r. For m^* the value $0.3m_e$ is used and the relative permittivity at low frequencies is taken as 9 (Hamberg and Granqvist 1986). Further, in the absence of tin, each impurity is assumed to be doubly charged, giving $Z = 2$ and $n = 2N_i$. The results of this calculation are shown in figure 2 by the broken line.

Elementary quantum mechanics (Merzbacher 1970) gives the condition for the validity of the first-order Born approximation for scattering from a screened Coulomb potential as

$$4k_F^2/\kappa_{TF}^2 > 1.$$

Plots of k_F, κ_{TF} and $4k_F^2/\kappa_{TF}^2$ using the parameters given above are shown in figure 4. It is clear that the Born approximation becomes less reliable as n is reduced.

Moore (1967) has calculated corrections to the first-order Born approximation by considering higher-order terms in the scattering and has obtained good agreement for the resistivity of n-type degenerate gallium arsenide over a range of carrier concentrations varying by a factor of about 100. Dingle's calculation, including Moore's corrections, is shown as the full line in figure 2. The overall calculation therefore reproduces well the experimental dependence of the resistivity on the carrier concentration for values of n between 10^{25} m^{-3} and 5×10^{26} m^{-3} although there is some evidence that the experimental points deviate above the calculation for values of n higher than 3×10^{26} m^{-3}. It is in this region that further calculations by Moore suggest that multiple scattering from pairs of defects may become important. This was neglected by Dingle.

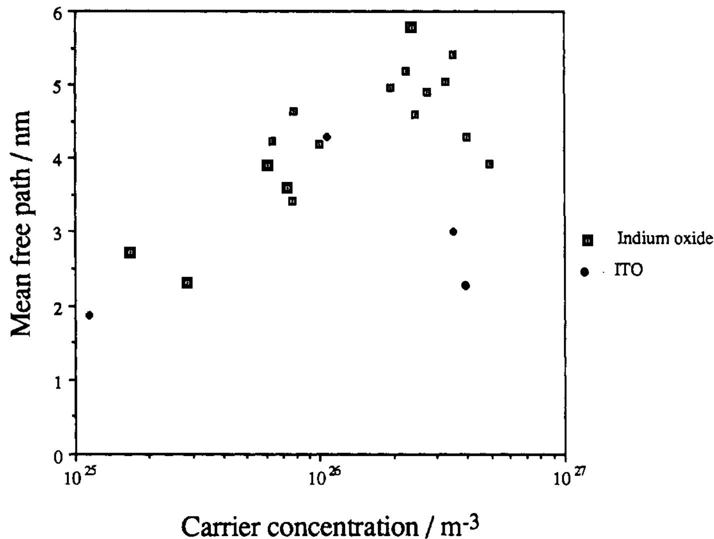

Figure 5. Electronic mean free path for all the samples shown in figure 2.

3.2. Comparison with crystalline data—the effect of the amorphous structure

It is clear from figure 2 that despite the amorphous structure of these films, the resistivity can be almost entirely accounted for by ionised impurity scattering, without any need to invoke scattering by the structural disorder. The weak effect of the amorphous structure is confirmed by comparison with the results shown in figure 2 for crystalline indium oxide films prepared by other workers. These data have been chosen as showing the lowest observed resistivity for any particular carrier concentration. It can be seen that the resistivity of the amorphous films is never more than twice that of the crystalline ones, and the difference is mostly less than this. The variation of the crystalline resistivity with carrier concentration is also in agreement with the trend of the ionised impurity scattering calculation.

It is not possible to be certain about the cause of the small difference between the amorphous and crystalline results. One possibility is that the crystalline films may have different values of m^* or ε_r or both. Equation (2) shows that m^*/ε_r need only vary by about 1.2 to produce the observed difference. This is within the scatter of values reported in the literature. The other possibility is that the difference is entirely due to scattering from structural disorder. This puts an upper limit on the contribution of this disorder to the resistivity. If the results are plotted as mean free path (figure 5) rather than as resistivity, a simple application of Matthiessen's rule gives a lower limit for the mean free path due to structural scattering of about 10 nm.

There is thus a clear contrast in the effect of structural disorder between orthodox amorphous metals and indium oxide. In the oxide the structure does no more than double the resistivity; the mean free path due to the structure is at least 10 nm. By contrast the resistivity of amorphous metals is typically $2 \times 10^{-6}\ \Omega$ m (Mooij 1973), about 100 times higher than a crystalline sample at room temperature, and the mean free path is typically the interatomic spacing.

The basic physics of this effect lies in the different wavelength of the electrons at the Fermi surface, which is about 3 nm in indium oxide and about 0.3 nm in aluminium. The

electrons in indium oxide are not scattered by the disorder because it varies rapidly on the scale of an electron wavelength and the electron sees only a smoothed out potential. This is not the case for metals where the electron wavelength is of the order of the interatomic spacing.

This argument can be put on a more formal basis. The rate of scattering of an electron from a state $\boldsymbol{k}$ to $\boldsymbol{k}'$ (both plane waves) is proportional to $|V(q)|^2$ where $V(q)$ is the Fourier component of the scattering potential at a wave vector $\boldsymbol{q}$ and $\boldsymbol{q}$ is equal to $\boldsymbol{k} - \boldsymbol{k}'$. For elastic scattering of a degenerate electron gas, the only q that can contribute to the scattering are given by $0 < q < 2k_F$. The general behaviour of $V(q)$ can be estimated from figure 1 which is broadly similar for indium oxide and amorphous metallic alloys. For indium oxide $2k_F$ is around 4 nm^{-1} but for a metallic alloy 20 to 30 nm^{-1} is typical. In the oxide only the region of low $V(q)$ can contribute to the scattering, but for an amorphous metal the region of the first large peak must be included, giving much stronger scattering.

Detailed calculations of structural scattering are beyond the scope of this paper but one further point can be made. It seems most likely that an increase in k_F will lead to stronger scattering off structural disorder as k_F slowly approaches the first peak in the structure factor. This may contribute to what appears to be an increasing divergence between the resistivities of amorphous and crystalline films at higher values of n in figure 2.

The conclusion of this section must be that, despite the amorphous structure, the electrons are only weakly scattered by the structural disorder, leading to a mean free path due to this source of scattering of at least 10 nm. The differences between the structural scattering in indium oxide and amorphous metals are consistent with simple ideas about the nature of the scattering from the disorder, but detailed calculations are not possible.

3.3. The effect of tin

Points marked with crosses on figure 2 were obtained from films prepared by sputtering a target containing 9% tin by weight, to provide a direct comparison between undoped and Sn-doped films of degenerate amorphous oxide. The films were prepared under conditions that were as similar as possible. This experiment has not previously been reported in the literature, where all the reports of amorphous transparent conductors prepared by ion beam sputtering have concentrated solely on ITO.

The first point that needs to be made about these ITO films is not shown in figure 2, but is made clear in figure 6. This plot of carrier concentration against oxygen partial pressure shows that the carrier concentration is controlled by the oxygen presence regardless of which target is used. This suggests that the presence of tin is not increasing the carrier concentration, contrary to the standard model of ITO presented in the introduction. According to this model, tin atoms should substitute for indium and should act as donors. If this model were applicable to these films there should be a contribution to the carrier concentration, independent of the oxygen partial pressure, and approximately equal to the density of tin atoms. If the composition of the films reflects the composition of the target then the density of tin atoms is about 3×10^{27} m^{-3}, which is 200 times higher than the lowest carrier concentration observed in these films. Although not consistent with the standard picture of the behaviour of tin in indium oxide these results are consistent with the work of another author (Fan 1979) who has observed a strong dependence of the carrier density on the oxygen pressure for films prepared by ion beam sputtering from a target containing about 10% SnO_2.

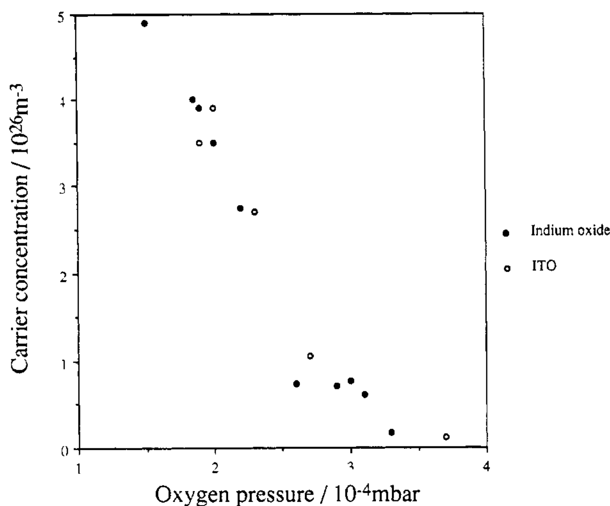

Figure 6. Carrier concentration for the indium oxide and ITO films as a function of the oxygen pressure at which they were prepared.

The conclusion that Sn is *not* effective as a dopant when the structure of the film is amorphous is also supported by the work of Gessert *et al* (1987) and Dhere *et al* (1987) who prepared amorphous ITO films by ion beam sputtering and then annealed them at successively higher temperatures. The effect was to change the structure of the film from amorphous to crystalline and to increase the carrier concentration by about $3 \times 10^{26}\,\mathrm{m}^{-3}$ and was interpreted as the tin atoms becoming effective as donors as the structure was changed. There is therefore a considerable amount of evidence for tin being ineffective as a donor in the amorphous films. There is, of course, considerable doubt over its role in crystalline films as well; the results of Fan *et al* (1977) for polycrystalline sputtered ITO films show a strong dependence of carrier concentration on the oxygen presence during sputtering.

The second question raised by the results of this work is why tin-doped films have higher resistivities than pure films with the same electron density when n is greater than about $2 \times 10^{26}\,\mathrm{m}^{-3}$. Data on this effect are a little sparse (see figure 2), but the observed resistivities of between $8 \times 10^{-6}\,\Omega\,\mathrm{m}$ and $10^{-5}\,\Omega\,\mathrm{m}$ are similar to those reported by Aharoni *et al* (1986) and Gessert *et al* (1987) for ion-beam-sputtered ITO films in this range of carrier concentration. If the tin is not ionised in these amorphous films then the results of the calculations for ionised impurity scattering off the oxygen vacancies should still apply. The electrons provided by ionised oxygen vacancies will still be scattered by those vacancies. It therefore seems that there may be an increase in the electron scattering due to the neutral tin impurities.

There is a third point concerning the effect of tin that results from the calculations presented above. The calculated resistivity due to ionised scattering is given by

$$\rho = [N_i Z^2 e^2 m^{*2} / 24\pi^3 (\varepsilon_0 \varepsilon_r)^2 \hbar^3 n^2] f(k_F).$$

Ignoring the slow variation of $f(k_F)$ this equation gives the mobility, μ, as

$$\mu = Bn/N_i Z^2$$

where B is a constant. This equation makes different predictions for the mobility in films

of indium oxide and ITO, if the standard model for the role of tin is correct. For pure indium oxide, with free electrons provided solely by oxygen vacancies, $Z = 2$ and $n = 2N_i$, giving $\mu = B/2$. For ITO, if the tin ions are providing the free electrons, $Z = 1$ and $n = N_i$, giving $\mu = B$. If these standard assumptions are correct, then the addition of tin should *increase* the mobility. This change in mobility has not been observed either here or by other authors who have prepared both types of film under the same conditions. Indeed Mizuhashi (1980), Ovadyahu *et al* (1983) and Hamberg and Granqvist (1986) have all observed lower mobilities when tin was added. These observations are more in line with a picture in which the carrier concentration is controlled largely by oxygen vacancies, and in which the tin may provide extra scattering centres, thereby decreasing the mobility.

The role of tin is therefore still not completely clear, despite 15 years of work on these films. Addition of tin undoubtedly increases the carrier concentration in crystalline films, as was observed by all the authors cited above, although it is not clear how carefully the oxygen conditions were controlled. The precise way in which this occurs, and how the electron scattering is affected remain uncertain. In amorphous films the position is clearer: it appears that the tin has no effect on the electron concentration, and may degrade the film by adding scattering centres.

4. Optical measurements

In order to investigate the basic optical properties of the transparent films, eight samples were prepared on silica substrates instead of the usual glass microscope slides. These were necessary because of the lower energy of the interband absorption edge in glass, which obscures the absorption due to the indium oxide film.

The eight samples consisted of four indium oxide and four ITO, with a range of carrier concentrations in each series. In each case a sample was simultaneously deposited in a geometry suitable for Hall effect measurements so that the carrier concentrations of the optical samples were known. The measurements of both transmission and absorption were made using a Perkin–Elmer λ-9 spectrometer in a standard two-beam configuration.

4.1. Transmission in the visible and near IR

Figure 7 shows the optical transmission of the film–substrate combination for each of the samples in the ITO series. Details of the optical samples are given in table 1. In the visible region of the spectrum the transmission is controlled by interference effects in the thin film. A peak is clearly seen at about 600 nm, while the trough at around 400 is partly obscured by the interband absorption.

The magnitude of the visible transmission, peaking just above 90%, compares well with crystalline samples where the same experiment has been performed. These amorphous films therefore have optical properties in the visible region that are as good as those of crystalline films prepared on heated substrates. The optical properties in the infra-red are controlled by the free electrons which give a high reflectivity at frequencies below the plasma frequency ω_p. It can be seen from figure 7 that the transmission falls at higher frequency as the carrier concentration is increased, in accordance with the change in the plasma frequency. Results for the series of pure indium oxide samples were similar implying that the optical properties of any particular film depend only on its carrier concentration and not on the presence or absence of tin.

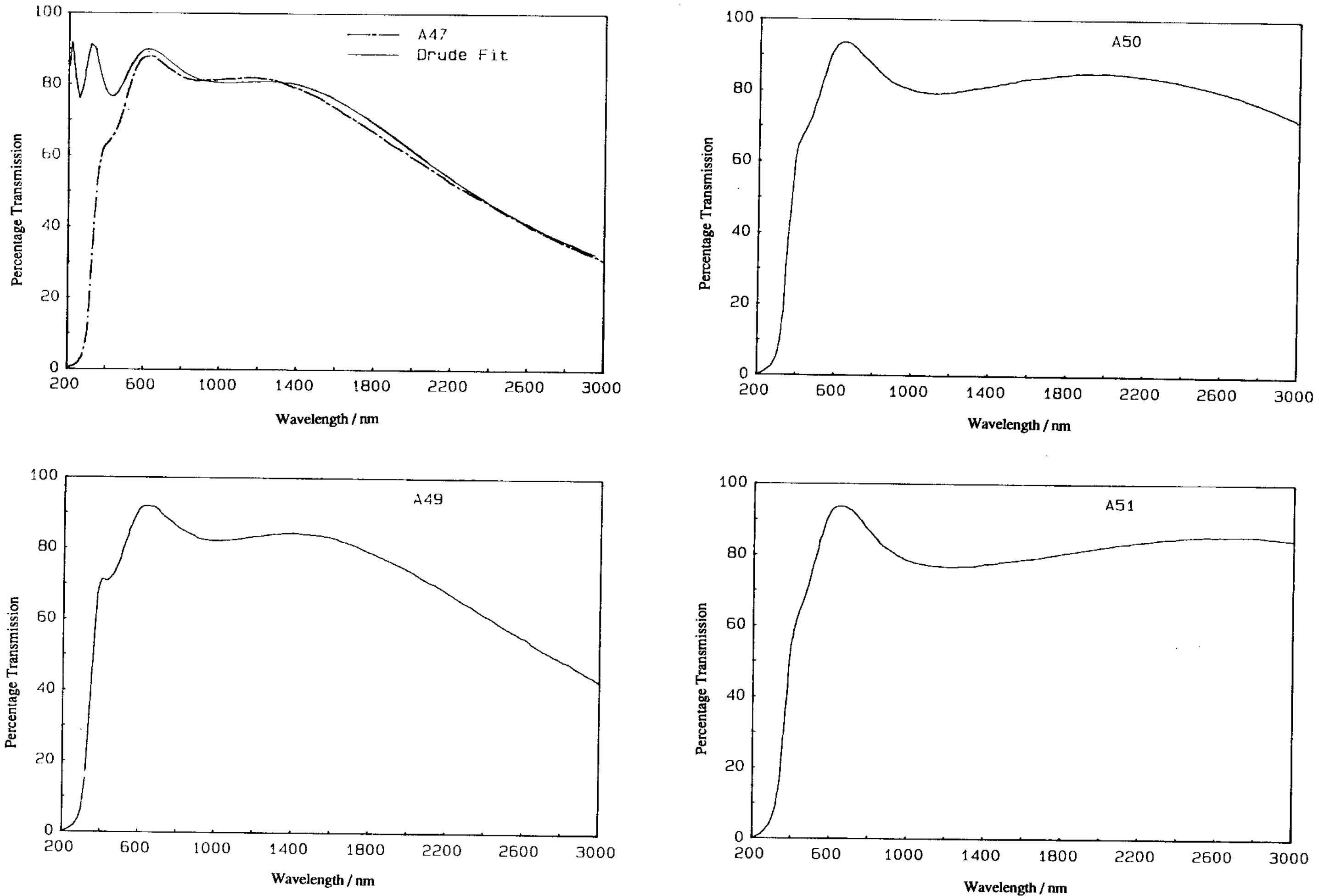

Figure 7. Optical transmission in the visible and near infra-red for the ITO samples. The data for A47 are shown with the fit obtained from the Drude calculations described in the text. The calculation is wrong at low wavelength because modelling of the interband absorption was not attempted.

Table 1. Details of the optical samples. A value of 4 was found for the high-frequency relative permittivity for all the fitted samples. The errors are estimated to be about 10% in the values for the effective mass and about 30% in the values for τ/m^*. IO denotes indium oxide without added tin.

Sample	Substance	Carrier density/m^{-3}	m^*/m_e	τ/m^*(opt)/s kg^{-1}	τ/m^*(DC)/s kg^{-1}
A38	IO	3.5×10^{26}	0.30	3×10^{16}	2.4×10^{16}
A37	IO	2.4×10^{26}	0.26	4×10^{16}	2.9×10^{16}
A39	IO	7.4×10^{25}			
A40	IO	Not degenerate			
A47	ITO	3.5×10^{26}	0.30	2×10^{16}	1.2×10^{16}
A49	ITO	2.7×10^{26}	0.28	3×10^{16}	2.2×10^{16}
A50	ITO	1.06×10^{26}			
A51	ITO	1.14×10^{25}			

The Drude theory of the optical properties was used to calculate the transmission of the film–substrate combination as a function of wavelength. This was done by calculating first the real and imaginary parts of the refractive index from the Drude theory and then the transmission at each wavelength using the known properties of the silica substrate. The matrix method of Heavens (1955) was used to take into account the multiple reflection and interference effects.

The two parameters put into the calculation were the carrier concentration, known from Hall effect measurements on simultaneously deposited material, and the film thickness. The high-frequency relative permittivity in the absence of free electrons, ε_∞, the effective mass and the electron scattering time were varied until the experimental results were reported. A typical fit is shown in figure 7. A value of 4 was found for ε_∞ for all the samples. Table 1 gives the value of m^* and τ which were extracted by this method for the samples that had strong plasma edges within the range of the spectrometer. Values of τ/m^* obtained this way are larger than values obtained from the low-frequency electrical measurements, as would be expected from the results of more sophisticated calculations (Gerlach and Grosse 1977, Hamberg and Granqvist 1986) of the frequency dependence of the ionised impurity scattering.

4.2. The absorption edge—the effect of the structure

The same spectrometer was used in its absorption mode to measure the absorption coefficient of the eight samples. Figure 8 shows the measurements from the samples with the highest and lowest carrier concentrations in both series. The other two samples are not shown to avoid confusing the diagram but were of similar form and were intermediate in position. An analysis of the errors has shown that these results for the absorption coefficient, α, are accurate to within a few per cent for $\alpha \geqslant 5 \times 10^4\ \mathrm{cm}^{-1}$, but that below this level the losses are dominated by multiple reflection and interference effects.

Figure 8 also shows data taken by Hamberg *et al* (1984) from a crystalline sample. Clearly the structure of the oxide has very little effect on the shape of the absorption edge.

Apart from the structural independence, it is hard to extract information from measurements of α against ω because there are several unknown factors that are required to model α. In principle α can be calculated from (see, e.g., Elliott 1984)

$$\alpha(\omega) = \frac{2}{n_0 c\omega}(2\pi e/m)^2 |P(\omega)|^2 \frac{1}{(2\pi)^3}\int_B \mathrm{d}^3\boldsymbol{k}\,\delta(E_f(\boldsymbol{k}) - E_i(\boldsymbol{k}) - \hbar\omega) \qquad (3)$$

where n_0 is the refractive index and c is the speed of light in vacuum. $|P(\omega)|^2$ is the square

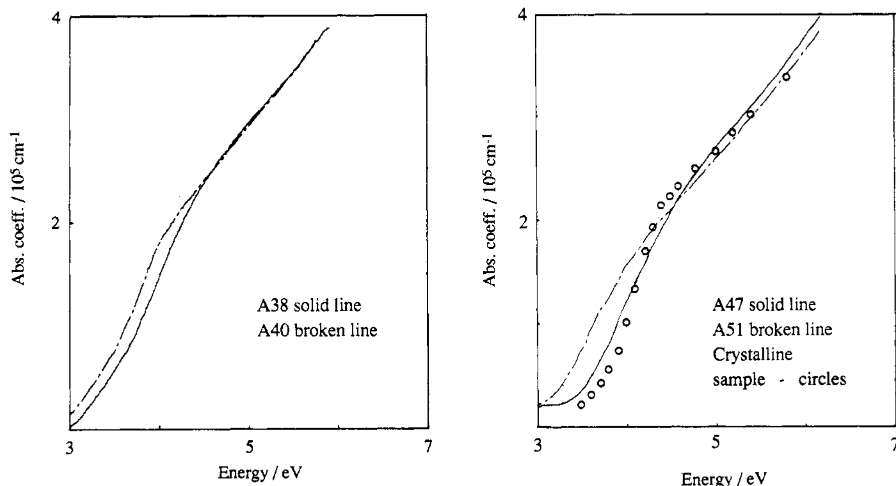

Figure 8. Optical absorption coefficients for samples of (left-hand panel) indium oxide and (right-hand panel) ITO. The carrier concentrations are given in table 1. The circles show data taken from a crystalline sample by Hamberg *et al* (1984).

of the matrix element linking initial and final states and is assumed independent of $\boldsymbol{k}$. The integral is taken over the Brillouin zone for crystalline materials but includes contributions only from transitions that conserve the momentum of the electron and are thus vertical on a conventional E–$\boldsymbol{k}$ diagram. Equation (3) shows that α will depend on details of the matrix elements and of the band structure, both of which are unknown, even for crystalline In_2O_3.

Simple assumptions for the form of the matrix elements and the band structure cannot explain the observed results. An obvious approximation is to assume an isotropic parabolic conduction band and matrix elements that vary slowly with energy, but to maintain the selection rule on $\boldsymbol{k}$. If the valence band is assumed to be relatively flat compared with the conduction band, as in SiO_2 or SnO_2 (Chelikowsky and Schlüter 1977, Robertson 1979), the integral gives the result

$$\omega\alpha(\omega) \propto (\hbar\omega - E_0)^{1/2}$$

where E_0 is the energy gap between the valence and conduction bands at $\boldsymbol{k} = 0$. The data for A40 are plotted as $\omega\alpha(\omega)$ against $\hbar\omega$ in figure 9. This sample was chosen as it had a highly activated resistivity which was several orders of magnitude higher than those of the other samples. Thus, in this sample, the effect of the blocking of transitions into filled conduction band states is minimised. It can be seen that the dependence is closer to being linear than of square root form. The simple assumptions on which this derivation was based are therefore not valid.

Amorphous indium oxide can also be contrasted with other amorphous semiconductors such as a-Si, As_2Te_3, As_2Se_3 and As_2S_3 which display (Mott and Davis 1979) parabolic absorption described by

$$\alpha(\omega) \propto (\hbar\omega - E_0)^2/\hbar\omega.$$

This behaviour has been explained by relaxing completely the requirement for $\boldsymbol{k}$-conservation. The integral over the Brillouin zone is replaced by a convolution of the densities of states in the valence and conduction bands:

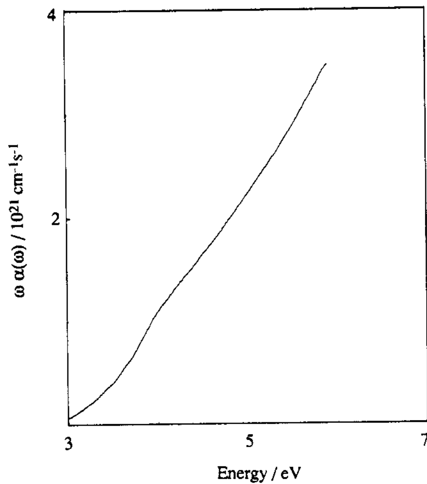

Figure 9. Absorption data for sample A40 plotted as $\omega\alpha(\omega)$ against energy.

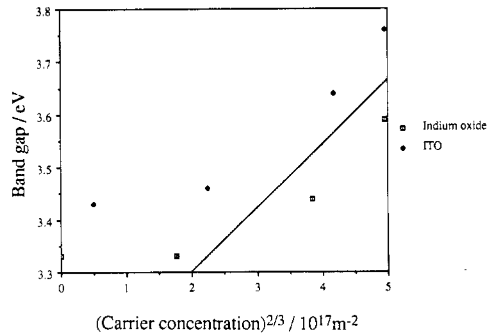

Figure 10. Band gap as a function of carrier concentration for the eight optical samples. The carrier concentration of A40 has been taken as zero for the purposes of this plot. The full line shows the gradient that would be expected for an effective mass of 0.3.

$$\omega\alpha(\omega) \propto \int N_{\mathrm{v}}(E)N_{\mathrm{c}}(E+\hbar\omega)\,\mathrm{d}E. \tag{4}$$

With the assumption of parabolic bands in both cases this integral gives the required parabolic form.

However, this argument cannot apply to the amorphous indium oxide studied here because the analysis of the resistivity and mean free path presented earlier shows that $\boldsymbol{k}$ is well defined with values of $\Delta k/k$ of between 0.1 and 0.2 for the films on which optical measurements were made. Momentum conservation will be only weakly relaxed and the Mott–Davis model cannot apply. The similarity of the electron scattering in the amorphous and crystalline cases is thus consistent with the similarity of the shape of the absorption edges in the two cases.

4.3. Absorption edges—shifts with carrier concentration

Figure 8 showed the absorption edges for pure indium oxide and ITO samples with the lowest and highest carrier concentrations. Intermediate samples showed similarly shaped edges in intermediate positions, so for both series there is a consistent shift towards higher energy as the carrier concentration is increased.

The mechanism for the shift was proposed independently by Moss and by Burstein in 1954. As the carrier concentration is increased, the conduction band is filled, so optically excited transitions from the valence band to the bottom of the conduction band are no longer possible. For a parabolic conduction band and a flat valence band the magnitude of the shift is given by

$$\Delta E_{\mathrm{BM}} = \hbar^2 k_{\mathrm{F}}^2/2m^* = [(3\pi^2)^{2/3}\hbar^2/2m^*]n^{2/3}.$$

As well as a shift in the position of the edge, this simple model also predicts a change

in the shape of the edge. If thermal smearing is ignored, then the density of states in the condiction band when transitions are first allowed will be greater for higher n, simply because of the $\sqrt{E}$ form of the density of states in the band. This should produce a sharper edge for samples with higher n.

The most commonly used approach to extracting the band gap is to use the fact that the plots of $\alpha(\omega)$ roughly follow the form $\alpha = \alpha_0(\hbar\omega - E_0)^{1/2}$. Thus α^2 is plotted against ω and a straight line is fitted to the region immediately above the edge. The band gap is taken to be the intercept of this line with the energy axis. This procedure cannot be justified theoretically but in the absence of a correct model for the shape and broadening of the edge, it has been used by several authors in order to follow movement of the edge (Vainshtein and Fistul' 1967, Ohhata *et al* 1979).

In order to compare the results with the predicted Moss–Burstein shift the values of the band gap obtained in this way are plotted against $n^{2/3}$ in figure 10. The straight line shows the gradient that would be expected for an effective mass of 0.3, assuming the valence band to be flat. The shifts of the gap at higher n are in reasonable agreement with the predictions but those at lower n are smaller than would be expected.

It is hard to be certain what is causing the reduced shift at lower n as there are various possible mechanisms. The first possibility is that the method for extracting the band gaps is not valid. This method takes no account of the fact that a change in the shape of the edge is predicted and therefore erroneous results may be produced by such a simple extraction method. The second possibility is that the parabolic model for the band is wrong at low values of n. The details of how the shape of the bottom of the conduction band varies as the doping is increased are not known. It is possible that both these effects are important.

To summarise, lack of knowledge of the band structure and the energy dependence of the matrix elements prevents a detailed modelling of the shape of the absorption edge. A detailed discussion of the shifts of the edge is difficult for the same reason. The overall shape of the edge is similar to that obtained for the crystalline material and this is consistent with the picture of the electron behaviour that emerged from the resistivity analysis.

5. Conclusions

The work described in this paper is the first detailed study of the physics of amorphous indium oxide. It has been shown that ion beam sputtering of a metal target in an oxygen atmosphere can produce amorphous films of conductivity and optical transparency equivalent to those of polycrystalline films produced on heated substrates. These amorphous films have important applications where substrates cannot be heated. As well as providing high-quality films on unheated substrates, ion beam sputtering has also allowed fine control of the carrier concentration in the films.

An analysis of the variation of resistivity with carrier concentration has shown that the resistivity can largely be accounted for by scattering of the electrons by the ionised impurities. The electrical properties are largely unaffected by the highly disordered structure due to the long wavelength of the electrons, which are consequently only weakly scattered by the disorder. The role of tin has also been investigated. In the amorphous material it does not appear to increase the carrier concentration, but may degrade the film by adding additional scattering centres and increasing the resistivity.

Optical studies have shown that the interband absorption is similar in amorphous and crystalline material, which is a consequence of the similarity of the electron scattering. It

has also been shown that Drude theory can account satisfactorily for the optical properties in the near infrared where the effects of the free-electron gas are important. The optical and electrical studies therefore together provide a consistent picture of the electron gas in this technically important and physically very interesting material.

Acknowledgments

We should like to thank Dr R Geere for performing the electron microscopy. We should also like to thank the SERC for a research grant and a studentship which supported one of us (JRB) during the course of this work.

References

Aharoni H, Coutts T J, Gessert T, Dhere R and Schilling L 1986 *J. Vac. Sci. Technol.* A **4** 428
Brooks H 1955 *Adv. Electron. Electron Phys.* **7** 85
Burstein E 1954 *Phys. Rev.* **93** 632
Chelikowsky J R and Schlüter M 1977 *Phys. Rev.* B **15** 4020
Chen T, Ma T P and Barker R C 1983 *Appl. Phys. Lett.* **43** 901
Dhere R G, Gessert T A, Schilling L L, Nelson A J, Jones K M, Aharoni H and Coutts T J 1987 *Solar Cells* **21** 281
Dingle R B 1955 *Phil. Mag.* **46** 831
Elliott S R 1984 *Physics of Amorphous Materials* (London: Longman)
Fan J C C 1979 *Appl. Phys. Lett.* **34** 515
Fan J C C, Bachner J and Foley G H 1977 *Appl. Phys. Lett.* **31** 773
Gerlach E and Grosse P 1977 *Festkörperprobleme (Advances in Solid State Physics)* vol 27 (Braunschweig: Vieweg) p 157
Gessert T A, Williamson D L, Coutts T J, Nelson A J, Jones K M, Dhere R G, Aharoni H and Zurcher P 1987 *J. Vac. Sci. Technol.* A **5** 1314
Hamberg I and Granqvist C G 1986 *J. Appl. Phys.* **60** R123
Hamberg I, Granqvist C G, Berggren K F, Sernelius B E and Engström L 1984 *Phys. Rev.* B **30** 3240
Heavens O S 1955 *Optical properties of Thin Solid Films* (Guildford: Butterworth)
Hebard A F and Nakahara S 1982 *Appl. Phys. Lett.* **41** 1130
Merzbacher E 1970 *Quantum Mechanics* (New York: Wiley)
Mizuhashi M 1980 *Thin Solid Films* **70** 91
Mooij J H 1973 *Phys. Status Solidi* a **17** 521
Moore E J 1967 *Phys. Rev.* **160** 618
Moss T S 1954 *Proc. Phys. Soc.* B **67** 775
Mott N F and Davis E A 1979 *Electronic Processes in Non-Crystalline Materials* (London: Oxford University Press)
Noguchi S and Sakata H 1980 *J. Phys. D: Appl. Phys.* **13** 1129
Ohhata Y, Shinoki F and Yoshida S 1979 *Thin Solid Films* **59** 255
Ovadyahu Z, Ovryn B and Kraner H W 1983 *J. Electrochem. Soc.* **130** 917
Pan C P and Ma T P 1980 *Appl. Phys. Lett.* **37** 163
Robertson J 1979 *J. Phys. C: Solid State Phys.* **12** 4767
Sadoc J F and Wagner C N J 1983 *Glassy Metals* vol 2 (Berlin: Springer)
Szczyrbowski J, Scmalzbauer K and Hoffman H 1986 *Thin Solid Films* **137** 169
Vainshtein V M and Fistul' V I 1967 *Sov. Phys.–Semicond.* **1** 104